*Calculation of B[superscript 0] → K[superscript *0]μ[superscript +]μ[superscript -] and B[0 over s] → #μ[superscript +]μ[superscript -] Observables Using Form Factors from Lattice QCD*

Calculation of $B^0 \to K^{*0}\mu^+\mu^-$ and $B_s^0 \to \phi\mu^+\mu^-$ Observables Using Form Factors from Lattice QCD

Ronald R. Horgan,[1] Zhaofeng Liu,[2] Stefan Meinel,[3,*] and Matthew Wingate[1]
[1]Department of Applied Mathematics and Theoretical Physics, University of Cambridge, Cambridge CB3 0WA, United Kingdom
[2]Institute of High Energy Physics and Theoretical Physics Center for Science Facilities, Chinese Academy of Sciences, Beijing 100049, China
[3]Center for Theoretical Physics, Massachusetts Institute of Technology, Cambridge, Massachusetts 02139, USA
(Received 24 October 2013; revised manuscript received 17 April 2014; published 30 May 2014)

We calculate the differential branching fractions and angular distributions of the rare decays $B^0 \to K^{*0}\mu^+\mu^-$ and $B_s^0 \to \phi\mu^+\mu^-$, using for the first time form factors from unquenched lattice QCD. We focus on the kinematic region where the K^* or ϕ recoils softly; there, the newly available form factors are most precise and the nonlocal matrix elements can be included via an operator product expansion. Our results for the differential branching fractions calculated in the standard model are higher than the experimental data. We consider the possibility that the deviations are caused by new physics and perform a fit of the Wilson coefficients C_9 and C_9' to the experimental data for multiple $B^0 \to K^{*0}\mu^+\mu^-$ and $B_s^0 \to \phi\mu^+\mu^-$ observables. In agreement with recent results from complementary studies, we obtain $C_9 - C_9^{\rm SM} = -1.0 \pm 0.6$ and $C_9' = 1.2 \pm 1.0$, whose deviations from zero would indicate the presence of nonstandard fundamental interactions.

DOI: 10.1103/PhysRevLett.112.212003 PACS numbers: 12.38.Gc, 13.20.He, 14.40.Nd

Decays involving the transition of a bottom quark to a strange quark are highly suppressed in the standard model. Contributions from nonstandard interactions could therefore be significant, causing observable changes in the decay rates and angular distributions. The search for such discrepancies is one of the most important routes to discovering what might lie beyond our current model of fundamental particle physics, and complements efforts to directly produce nonstandard particles. Because of quark confinement, the $b \to s$ transitions are being observed with hadronic initial and final states. Among the cases that have been measured experimentally [1], the decay $B \to K^*\ell^+\ell^-$, (where ℓ is an electron or muon) is proving to be particularly powerful in looking for physics beyond the standard model [2–13].

The LHCb Collaboration recently published new precision measurements of the decay $B \to K^*\mu^+\mu^-$, and one of the observables shows a significant deviation from the standard model predictions [14]. There is currently an intense effort to understand this discrepancy, which could be a manifestation of new physics [15–22]. Previous calculations of the matrix elements that relate the underlying $b \to s$ interactions and the hadronic observables are reliable only in the kinematic region of high recoil (large K^* momentum in the B rest frame), and consequently it was in this region that a discrepancy was found. In the low-recoil region, numerical lattice QCD computations must be performed. We recently completed the first unquenched lattice QCD calculation of the form factors that parametrize the hadronic matrix elements relevant for $B \to K^*\ell^+\ell^-$ and $B_s \to \phi\ell^+\ell^-$ [23]. In this Letter, we investigate the consequences of using these results in combination with experimental data. We find that hints of deviations from the standard model are present also in the low-recoil region, and a better fit of the data is obtained by allowing nonstandard interactions consistent with those suggested to explain the aforementioned anomaly at high recoil.

At hadronic energy scales, $b \to s\gamma$ and $b \to s\ell^+\ell^-$ transitions can be described using an effective Hamiltonian of the form [24–31]

$$\mathcal{H}_{\rm eff} = -\frac{4G_F}{\sqrt{2}} V_{tb} V_{ts}^* \sum_i [C_i O_i + C_i' O_i'], \tag{1}$$

where $O_i^{(\prime)}$ are local operators and $C_i^{(\prime)}$ are the corresponding Wilson coefficients, encoding the physics at the electroweak energy scale and beyond. The operators

$$O_7^{(\prime)} = e m_b/(16\pi^2) \bar{s}\sigma_{\mu\nu} P_{R(L)} b F^{\mu\nu}, \tag{2}$$

$$O_9^{(\prime)} = e^2/(16\pi^2) \bar{s}\gamma_\mu P_{L(R)} b \bar{\ell}\gamma^\mu \ell, \tag{3}$$

$$O_{10}^{(\prime)} = e^2/(16\pi^2) \bar{s}\gamma_\mu P_{L(R)} b \bar{\ell}\gamma^\mu \gamma_5 \ell, \tag{4}$$

where $F^{\mu\nu}$ is the electromagnetic field strength tensor, give the leading contributions to the decays we will discuss in this work. The operators $O_{1...6}^{(\prime)}$ are four-quark operators, and $O_8^{(\prime)}$ contains the gluon field strength tensor. The primed operators differ from the unprimed operators in their chirality [$P_{R,L} = (1 \pm \gamma_5)/2$]; the standard model predicts that their Wilson coefficients, C_i', are negligibly small.

The utility of the decay $B \to K^*(\to K\pi)\ell^+\ell^-$ is that all six Dirac structures in Eqs. (2)–(4) have nonzero matrix elements, and the angular distribution can be used to disentangle them. In the narrow-width approximation [32,33], the kinematics of the quasi-four-body decay $\bar{B}^0 \to \bar{K}^{*0}(\to K^-\pi^+)\ell^+\ell^-$ is described by four variables: the invariant mass of the lepton pair, q^2, and the three angles θ_ℓ, θ_{K^*}, ϕ, defined here as in Ref. [2]. In this approximation, the general form of the decay distribution is [2,32–35]

$$\frac{d^4\Gamma}{dq^2 d\cos\theta_\ell d\cos\theta_{K^*} d\phi} = \frac{9}{32\pi}[I_1^s \sin^2\theta_{K^*} + I_1^c \cos^2\theta_{K^*} + (I_2^s \sin^2\theta_{K^*} + I_2^c \cos^2\theta_{K^*})\cos 2\theta_\ell + I_3 \sin^2\theta_{K^*}\sin^2\theta_\ell \cos 2\phi$$
$$+ I_4 \sin 2\theta_{K^*} \sin 2\theta_\ell \cos\phi + I_5 \sin 2\theta_{K^*} \sin\theta_\ell \cos\phi + (I_6^s \sin^2\theta_{K^*} + I_6^c \cos^2\theta_{K^*})\cos\theta_\ell$$
$$+ I_7 \sin 2\theta_{K^*} \sin\theta_\ell \sin\phi + I_8 \sin 2\theta_{K^*} \sin 2\theta_\ell \sin\phi + I_9 \sin^2\theta_{K^*}\sin^2\theta_\ell \sin 2\phi], \quad (5)$$

where the coefficients $I_i^{(a)}$ depend only on q^2. Integrating over the angles, one obtains the differential decay rate $d\Gamma/dq^2 = \frac{3}{4}(2I_1^s + I_1^c) - \frac{1}{4}(2I_2^s + I_2^c)$. The angular distribution of the CP-conjugated mode $B^0 \to K^{*0}(\to K^+\pi^-)\ell^+\ell^-$ is obtained from Eq. (5) through the replacements $I_{1,2,3,4,7}^{(a)} \to \bar{I}_{1,2,3,4,7}^{(a)}$, $I_{5,6,8,9}^{(a)} \to -\bar{I}_{5,6,8,9}^{(a)}$ [2]. Normalized CP averages and CP asymmetries of the angular coefficients are then defined as follows [2]:

$$S_i^{(a)} = \frac{I_i^{(a)} + \bar{I}_i^{(a)}}{d(\Gamma + \bar{\Gamma})/dq^2}, \qquad A_i^{(a)} = \frac{I_i^{(a)} - \bar{I}_i^{(a)}}{d(\Gamma + \bar{\Gamma})/dq^2}. \quad (6)$$

The experiments actually yield results for binned observables $\langle S_i^{(a)} \rangle$ and $\langle A_i^{(a)} \rangle$, given by the ratios of q^2 integrals of numerator and denominator in Eq. (6).

The observables $\langle S_{4,5,7,8} \rangle$ and the ratios,

$$\langle P'_{4,5,6,8} \rangle = \frac{\langle S_{4,5,7,8} \rangle}{2\sqrt{-\langle S_2^c \rangle \langle S_2^s \rangle}}, \quad (7)$$

(note the different indices on the left-hand and right-hand sides) have recently been measured for the first time by the LHCb Collaboration in the decay $\bar{B}^0 \to \bar{K}^{*0}(\to K^-\pi^+)\mu^+\mu^-$ (and its CP conjugate) [14]. The ratios (7) are designed to reduce hadronic uncertainties at low q^2 [36]. For P_5', a significant discrepancy between the LHCb result and the standard model prediction of Ref. [37] was found in the bin $4.30\ \mathrm{GeV}^2 \le q^2 \le 8.68\ \mathrm{GeV}^2$ [14]. In Ref. [15] it was suggested that this discrepancy, as well as some smaller deviations in other observables, can be explained by a negative new-physics (NP) contribution to the Wilson coefficient C_9; specifically, $C_9 = C_9^{\mathrm{SM}} + C_9^{\mathrm{NP}}$, where $C_9^{\mathrm{SM}} \approx 4$ is the standard model value and $C_9^{\mathrm{NP}} \approx -1.5$. The authors of Ref. [16] performed global fits of the latest experimental data in multiple $b \to s$ decay channels, allowing various subsets of the Wilson coefficients to deviate from their respective standard model values. Allowing two Wilson coefficients to deviate, the biggest reduction in χ^2 was obtained for

$$C_9^{\mathrm{NP}} = -1.0 \pm 0.3, \qquad C_9' = 1.0 \pm 0.5. \quad (8)$$

Such large effects in C_9 and C_9' can arise in models with flavor-changing neutral gauge bosons (Z') in the few-TeV mass range [15–17,19,20], and in models that generate new four-quark operators of scalar and pseudoscalar type [21].

Extractions of Wilson coefficients from the experimental data require knowledge of the matrix elements of the operators $O_i^{(\prime)}$ in nonperturbative QCD. The analyses discussed above are based on calculations of the $B \to K^*$ matrix elements using light-cone sum rules [38–40] and QCD factorization [41]. These calculations are limited to the low-q^2 (high recoil) region. On the other hand, the experiments cover the entire kinematic range $4m_\ell^2 < q^2 < (m_B - m_{K^*})^2 \approx 19\ \mathrm{GeV}^2$, and changes in $C_9^{(\prime)}$ will also affect the high-q^2 region. We have recently completed the first lattice QCD calculation of the complete set of form factors giving the $B \to K^*$ and $B_s \to \phi$ matrix elements of the operators $O_7^{(\prime)}$, $O_9^{(\prime)}$, and $O_{10}^{(\prime)}$ in the high-q^2 region [23]. In the following, we use these results to calculate the differential branching fractions and the angular observables for the decays $\bar{B}^0 \to \bar{K}^{*0}(\to K^-\pi^+)\mu^+\mu^-$ and $\bar{B}_s^0 \to \phi(\to K^-K^+)\mu^+\mu^-$.

In the narrow-width approximation, the $\bar{B}^0 \to K^-\pi^+\mu^+\mu^-$ decay amplitude can be written in terms of the $\bar{B}^0 \to \bar{K}^{*0}\mu^+\mu^-$ decay amplitude as explained in Ref. [32]. This amplitude takes the form

$$\mathcal{M} = \frac{G_F \alpha}{\sqrt{2}\pi} V_{tb} V_{ts}^* [(\mathcal{A}_\mu + \mathcal{T}_\mu)\bar{u}_\ell \gamma^\mu v_\ell + \mathcal{B}_\mu \bar{u}_\ell \gamma^\mu \gamma_5 v_\ell], \quad (9)$$

with the local hadronic matrix elements,

$$\mathcal{A}_\mu = -\frac{2m_b}{q^2} q^\nu \langle \bar{K}^* | \bar{s} i\sigma_{\mu\nu}(C_7 P_R + C_7' P_L) b | \bar{B} \rangle$$
$$+ \langle \bar{K}^* | \bar{s}\gamma_\mu (C_9 P_L + C_9' P_R) b | \bar{B} \rangle, \quad (10)$$

$$\mathcal{B}_\mu = \langle \bar{K}^* | \bar{s}\gamma_\mu (C_{10} P_L + C_{10}' P_R) b | \bar{B} \rangle, \quad (11)$$

and the nonlocal hadronic matrix element,

$$\mathcal{T}_\mu = \frac{-16i\pi^2}{q^2} \sum_{i=1\ldots6;8} C_i \int d^4x e^{iq\cdot x} \langle \bar{K}^* | \mathrm{T} O_i(0) j_\mu(x) | \bar{B} \rangle. \tag{12}$$

In Eq. (12), $j_\mu(x)$ denotes the quark electromagnetic current. Near $q^2 = m^2_{J/\psi(1S)}, m^2_{\psi(2S)}$, the contributions from O_1 and O_2 in $\mathcal{T}_\mu$ are resonantly enhanced, preventing reliable theoretical calculations in these regions. At high q^2 ($\sim m_b^2$), $\mathcal{T}_\mu$ can be expanded in an operator product expansion (OPE), with the result [42],

$$\begin{aligned}\mathcal{T}_\mu = &-T_7(q^2)\frac{2m_b}{q^2} q^\nu \langle \bar{K}^* | \bar{s} i \sigma_{\mu\nu} P_R b | \bar{B} \rangle \\ &+ T_9(q^2) \langle \bar{K}^* | \bar{s}\gamma_\mu P_L b | \bar{B} \rangle + \frac{1}{2q^2} \sum_{i=1}^{5} B_i \langle \bar{K}^* | O^{(-1)}_{i\mu} | \bar{B} \rangle \\ &+ \mathcal{O}(\Lambda^2/m_b^2, m_c^4/q^4).\end{aligned} \tag{13}$$

(See also Ref. [43] for an alternative version of the OPE.) In Eq. (13), the $O^{(-1)}_{i\mu}$ are dimension-four operators containing a derivative, and $T_{7,9}(q^2) = C^{\mathrm{eff}}_{7,9}(q^2) - C_{7,9}$ with $C^{\mathrm{eff}}_{7,9}(q^2)$ given by Eqs. (3.9) and (3.10) of Ref. [4].

The matrix elements $\langle \bar{K}^* | \bar{s}\Gamma b | \bar{B} \rangle$ (and analogously for $\bar{B}_s \to \phi$) in Eqs. (10), (11), and (13) can be written in terms of the seven form factors V, A_0, A_1, A_{12}, T_1, T_2, and T_{23} [23]. We describe the dependence of the form factors on q^2 using the simplified series expansion [44]. The corresponding parameters were obtained by fitting the lattice QCD data, and are given in Tables VII– XI of Ref. [23]. The matrix elements of the dimension-four operators in Eq. (13) have not yet been calculated in lattice QCD, and we will neglect this term. This introduces a small systematic uncertainty of order $\alpha_s \Lambda / m_b \sim 2\%$ [42].

We take the standard model values of the Wilson coefficients $C_{1,2,\ldots,10}$, calculated at next-to-next-to-leading-logarithmic order, from Ref. [2]. Following the same reference, we set $\alpha_s(m_b) = 0.214$, $m_c(m_c) = 1.3$ GeV, and $m_b(m_b) = 4.2$ GeV. We evaluate the electromagnetic coupling at $\mu = m_b$, corresponding to $\alpha = 1/133$, which minimizes higher-order electroweak corrections [45]. We take the hadron masses from the Particle Data Group [46] and use the mean life times $\tau_{B^0} = 1.519(7)$ ps and $\tau_{B_s^0} = 1.516(11)$ ps from Ref. [1]. We take $|V_{tb}V^*_{ts}| = 0.040\,88(57)$ from the Summer 2013 standard model fit of Ref. [47].

While the decay $\bar{B}^0 \to \bar{K}^{*0}(\to K^-\pi^+)\mu^+\mu^-$ is self-tagging, the final state of $\bar{B}_s^0 \to \phi(\to K^-K^+)\ell^+\ell^-$ does not determine whether it resulted from the decay of a $\bar{B}_s^0$ or a B_s^0 meson. Therefore, we calculate the time-integrated untagged average over the $\bar{B}_s^0$ and B_s^0 decay distributions, including the effects of $\bar{B}_s^0$-B_s^0 mixing as explained in Ref. [48]. We use the width difference $\Delta\Gamma_s = 0.081(11)\ \mathrm{ps}^{-1}$ [1].

Our results for the differential branching fractions $d\mathcal{B}/dq^2 = \tau_{B^0_{(s)}}\, d\Gamma/dq^2$ and the angular observables F_L, S_3, S_4, P'_4, S_5, P'_5, A_{FB}, where $F_L = -S_2^c$ and $A_{FB} = (-3/8)(2S_6^s + S_6^c)$, are shown in Fig. 1 (the observables $S_{7,8,9}$ as well as the CP asymmetries $A_i^{(a)}$ are expected to be close to zero in the standard model). The shaded bands in Fig. 1 indicate the total theoretical uncertainty,

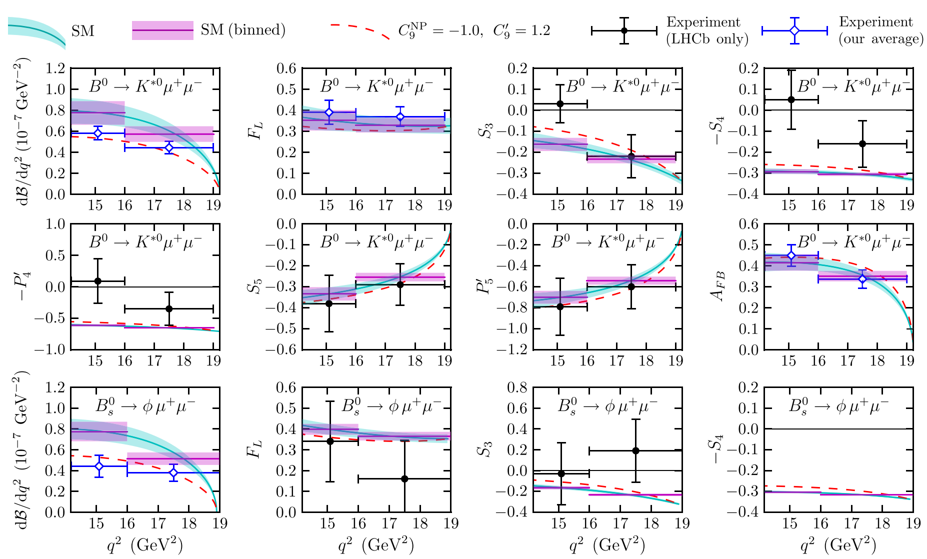

FIG. 1 (color online). Observables for the decays $B^0 \to K^{*0}\mu^+\mu^-$ (upper two rows) and $B_s^0 \to \phi\mu^+\mu^-$ (bottom row: untagged averages over the $\bar{B}_s^0$ and B_s^0 distributions). The solid curves show our theoretical results in the standard model; the shaded areas give the corresponding total uncertainties (with and without binning). The dashed curves correspond to the new-physics fit result $C_9 = C_9^{\mathrm{SM}} - 1.0$, $C'_9 = 1.2$ (the uncertainties of the dashed curves are not shown for clarity). We also show our averages of results from the CDF, LHCb, CMS, and ATLAS experiments [14,51–53,55] (note that $S_4^{(\mathrm{LHCb})} = -S_4$ and $P_4'^{(\mathrm{LHCb})} = -P'_4$).

originating from the following sources: the form factor uncertainties [23], an estimated 2% uncertainty in the values of the Wilson coefficients C_i [49], the uncertainties in the B^0 and B_s^0 meson mean life times, the uncertainty in $|V_{tb}V_{ts}^*|$, and an estimated additional 5% systematic uncertainty in the vector amplitude ($\mathcal{A}_\mu + \mathcal{T}_\mu$) in Eq. (9), which is introduced by the truncation of the OPE and duality violations [42,43]. Note that S-wave pollution is expected to be negligible at large q^2 [50].

In Fig. 1, we also show experimental results, which are given for the bins 14.18 GeV$^2 < q^2 <$ 16 GeV^2 (bin 1) and 16 GeV$^2 < q^2 <$ 19 GeV^2 (bin 2). Some of the observables have only been measured by LHCb [14,51,52]. For the $B_s^0 \to \phi\mu^+\mu^-$ branching fraction, we averaged the results from LHCb [52] and CDF [53]. For the $B^0 \to K^{*0}\mu^+\mu^-$ branching fraction, we averaged the results from LHCb [51], CMS [54], and CDF (bin 1 only, due to different upper q^2 limit in bin 2) [53]. For A_{FB} and F_L, we additionally included the ATLAS results [55] in the average. Our binned theoretical results are given in Table I and are also shown in Fig. 1.

We find that our standard model results for the differential branching fractions of both $B^0 \to K^{*0}\mu^+\mu^-$ and $B_s^0 \to \phi\mu^+\mu^-$ are about 30% higher than the experimental data. Note that for $B_s^0 \to \phi\mu^+\mu^-$, a higher-than-observed differential branching fraction was also found using form factors from light-cone sum rules [39] (see Fig. 3 of Ref. [52]) and from a relativistic quark model [56]. In the high-q^2 region considered here, our results for the observables F_L, S_5, P_5', and A_{FB} are in agreement with experiment. For the $B^0 \to K^{*0}\mu^+\mu^-$ observables S_3, S_4, and P_4', we see deviations between the LHCb data and our results in bin 1, in agreement with Refs. [16,18].

To study the possibility of new physics in the Wilson coefficients C_9 and C_9', we performed a fit of these two parameters to the experimental data above $q^2 = 14.18$ GeV^2, keeping all other Wilson coefficients fixed at their standard model values (and assuming C_9, $C_9' \in \mathbb{R}$). We included the observables $\mathrm{d}\mathcal{B}/\mathrm{d}q^2$, F_L, S_3, S_4, S_5, A_{FB} for $B^0 \to K^{*0}\mu^+\mu^-$, and $\mathrm{d}\mathcal{B}/\mathrm{d}q^2$, F_L, S_3 for $B_s^0 \to \phi\mu^+\mu^-$. We fully took into account the correlations between our theoretical results for different observables and different bins. The best-fit values are

$$C_9^{\rm NP} = -1.0 \pm 0.6, \qquad C_9' = 1.2 \pm 1.0, \qquad (14)$$

and the likelihood function is plotted in Fig. 2. The dashed curves in Fig. 1 show the observables evaluated at the best-fit values. To investigate how much the uncertainties in Eq. (14) are influenced by the theoretical and experimental uncertainties, we performed new fits where we artificially eliminated or reduced different sources of uncertainty. In particular, setting all form factor uncertainties to zero results in $C_9^{\rm NP} = -0.9 \pm 0.4$, $C_9' = 0.7 \pm 0.5$, and raises the statistical significance for nonzero ($C_9^{\rm NP}$, C_9') from 2σ to 3σ. Reducing instead the experimental uncertainties can have a more dramatic effect, because some of the angular observables already have very small theory uncertainties compared to the current experimental uncertainties.

Our result (14) is in remarkable agreement with the result (8) of the fit performed in Ref. [16], which did not include the $B_s^0 \to \phi\mu^+\mu^-$ data. Equation (14) is also consistent with the value $C_9^{\rm NP} \sim -1.5$ obtained in Ref. [15], and with the very recent Bayesian analysis of Ref. [22]. As expected [16,18], the new-physics scenario (14) does not remove the tension seen in bin 1 for S_4/P_4'. Nevertheless, the fit (14) significantly improves the overall agreement with the data, reducing the total χ^2 by 5.7 and giving $\chi^2/\mathrm{d.o.f.} = 0.96$. We also performed a fit of the experimental data for all observables in bin 2 only, which gives

TABLE I. Binned theoretical results in the standard model, for the two q^2 ranges specified in the header of the table (in GeV^2). The uncertainties given here are the total uncertainties, as explained in the main text.

Observable	[14.18, 16.00]	[16.00, 19.00]
$B^0 \to K^{*0}\mu^+\mu^-$		
$\langle \mathrm{d}\mathcal{B}/\mathrm{d}q^2 \rangle$ (10^{-7} GeV^{-2})	0.77(11)	0.569(74)
$\langle F_L \rangle$	0.352(49)	0.329(35)
$\langle S_3 \rangle$	−0.163(31)	−0.233(20)
$\langle S_4 \rangle$	0.292(12)	0.3051(84)
$\langle P_4' \rangle$	0.613(18)	0.6506(84)
$\langle S_5 \rangle$	−0.333(32)	−0.253(20)
$\langle P_5' \rangle$	−0.700(61)	−0.539(38)
$\langle A_{FB} \rangle$	0.414(38)	0.350(25)
$B_s^0 \to \phi\mu^+\mu^-$		
$\langle \mathrm{d}\mathcal{B}/\mathrm{d}q^2 \rangle$ (10^{-7} GeV^{-2})	0.775(94)	0.517(60)
$\langle F_L \rangle$	0.398(26)	0.365(21)
$\langle S_3 \rangle$	−0.166(16)	−0.233(12)
$\langle S_4 \rangle$	0.3039(51)	0.3164(38)
$\langle P_4' \rangle$	0.6223(91)	0.6582(46)

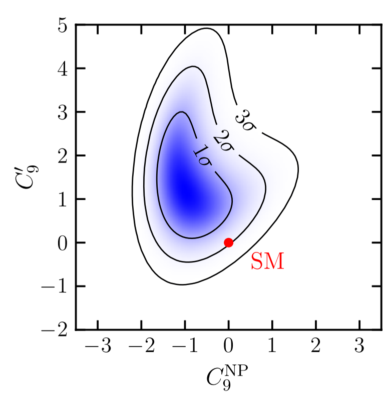

FIG. 2 (color online). The likelihood function of a fit to the $B^0 \to K^{*0}\mu^+\mu^-$ and $B_s^0 \to \phi\mu^+\mu^-$ experimental data above $q^2 = 14.18$ GeV^2, with fit parameters $C_9^{\rm NP}$ and C_9'. The contours correspond to $\Delta\chi^2 = 2.30$, 6.18, 11.83.

$$C_9^{\rm NP} = -0.9 \pm 0.7, \quad C_9' = 0.4 \pm 0.7 \ \ (\text{bin 2 only}). \quad (15)$$

A major concern about the calculations is the possibility of larger-than-expected contributions from broad charmonium resonances above the $\psi(2S)$. In the $B^+ \to K^+\mu^+\mu^-$ differential decay rate, the LHCb Collaboration recently reported sizable peaks associated with the $\psi(3770)$ and $\psi(4160)$ [57]. Note that the OPE which we use to include $c\bar{c}$ effects [Eq. (13)] is expected to describe only q^2-integrated observables (in the high-q^2 region) [43]. To test the robustness of our analysis, we added Breit-Wigner amplitudes with the masses and widths of the $\psi(3770)$ and $\psi(4160)$ [58] to $T_9(q^2)$, and included their complex-valued couplings as nuisance parameters. We constrained the magnitudes of these couplings to allow the ratios of the purely resonant and nonresonant contributions to the differential decay rates at $q^2 = m^2_{\psi(3770)}$ and $q^2 = m^2_{\psi(4160)}$ to be as large as in Fig. 1 of Ref. [57], but we left the phases unconstrained. A fit of $C_9^{\rm NP}$, C_9' in the presence of these nuisance parameters gives $C_9^{\rm NP} = -1.1 \pm 0.7$, $C_9' = 1.2 \pm 1.1$; the significance for nonzero ($C_9^{\rm NP}$, C_9') gets reduced to 1.4σ. We stress that adding Breit-Wigner amplitudes is model-dependent and corresponds to a double counting of the $c\bar{c}$ degrees of freedom. A better understanding of the resonant contributions from first-principles QCD is needed.

We gratefully acknowledge discussions with Wolfgang Altmannshofer, William Detmold, Gudrun Hiller, Alexander Lenz, Joaquim Matias, Iain W. Stewart, Jesse Thaler, and Michael Williams. S. M. is supported by the U.S. Department of Energy under cooperative research agreement Contract No. DE-FG02-94ER40818. This work was supported in part by an STFC Special Programme Grant (PP/E006957/1). R. H. and M. W. are supported by an STFC Consolidated Grant. Z. L. is partially supported by NSFC under the Project No. 11105153, the Youth Innovation Promotion Association of CAS, and the Scientific Research Foundation for ROCS, SEM.

*smeinel@mit.edu

[1] Y. Amhis *et al.* (Heavy Flavor Averaging Group), arXiv:1207.1158; online updates available at http://www.slac.stanford.edu/xorg/hfag/.
[2] W. Altmannshofer, P. Ball, A. Bharucha, A. J. Buras, D. M. Straub, and M. Wick, J. High Energy Phys. 01 (2009) 019.
[3] A. K. Alok, A. Dighe, D. Ghosh, D. London, J. Matias, M. Nagashima, and A. Szynkman, J. High Energy Phys. 02 (2010) 053.
[4] C. Bobeth, G. Hiller, and D. van Dyk, J. High Energy Phys. 07 (2010) 098.
[5] A. K. Alok, A. Datta, A. Dighe, M. Duraisamy, D. Ghosh, and D. London, J. High Energy Phys. 11 (2011) 121.
[6] A. K. Alok, A. Datta, A. Dighe, M. Duraisamy, D. Ghosh, and D. London, J. High Energy Phys. 11 (2011) 122.
[7] C. Bobeth, G. Hiller, and D. van Dyk, J. High Energy Phys. 07 (2011) 067.
[8] D. Bećirević and E. Schneider, Nucl. Phys. **B854**, 321 (2012).
[9] W. Altmannshofer, P. Paradisi, and D. M. Straub, J. High Energy Phys. 04 (2012) 008.
[10] J. Matias, F. Mescia, M. Ramon, and J. Virto, J. High Energy Phys. 04 (2012) 104.
[11] F. Beaujean, C. Bobeth, D. van Dyk, and C. Wacker, J. High Energy Phys. 08 (2012) 030.
[12] W. Altmannshofer and D. M. Straub, J. High Energy Phys. 08 (2012) 121.
[13] C. Bobeth, G. Hiller, and D. van Dyk, Phys. Rev. D **87**, 034016 (2013).
[14] R. Aaij *et al.* (LHCb Collaboration), Phys. Rev. Lett. **111**, 191801 (2013).
[15] S. Descotes-Genon, J. Matias, and J. Virto, Phys. Rev. D **88**, 074002 (2013).
[16] W. Altmannshofer and D. M. Straub, Eur. Phys. J. C **73**, 2646 (2013).
[17] R. Gauld, F. Goertz, and U. Haisch, Phys. Rev. D **89**, 015005 (2014).
[18] C. Hambrock, G. Hiller, S. Schacht, and R. Zwicky, Phys. Rev. D **89**, 074014 (2014).
[19] A. J. Buras and J. Girrbach, J. High Energy Phys. 12 (2013) 009.
[20] R. Gauld, F. Goertz, and U. Haisch, J. High Energy Phys. 01 (2014) 069.
[21] A. Datta, M. Duraisamy, and D. Ghosh, Phys. Rev. D **89**, 071501 (2014).
[22] F. Beaujean, C. Bobeth, and D. van Dyk, arXiv:1310.2478.
[23] R. R. Horgan, Z. Liu, S. Meinel, and M. Wingate, Phys. Rev. D **89**, 094501 (2014).
[24] B. Grinstein, M. J. Savage, and M. B. Wise, Nucl. Phys. **B319**, 271 (1989).
[25] B. Grinstein, R. P. Springer, and M. B. Wise, Nucl. Phys. **B339**, 269 (1990).
[26] M. Misiak, Nucl. Phys. **B393**, 23 (1993); **B439**, 461(E) (1995).
[27] A. J. Buras, M. Misiak, M. Münz, and S. Pokorski, Nucl. Phys. **B424**, 374 (1994).
[28] A. J. Buras and M. Münz, Phys. Rev. D **52**, 186 (1995).
[29] G. Buchalla, A. J. Buras, and M. E. Lautenbacher, Rev. Mod. Phys. **68**, 1125 (1996).
[30] K. G. Chetyrkin, M. Misiak, and M. Münz, Phys. Lett. B **400**, 206 (1997); **425**, 414(E) (1998).
[31] C. Bobeth, M. Misiak, and J. Urban, Nucl. Phys. **B574**, 291 (2000).
[32] F. Krüger, L. M. Sehgal, N. Sinha, and R. Sinha, Phys. Rev. D **61**, 114028 (2000); **63**, 019901(E) (2000).
[33] C. S. Kim, Y. G. Kim, C.-D. Lü, and T. Morozumi, Phys. Rev. D **62**, 034013 (2000).
[34] A. Faessler, T. Gutsche, M. A. Ivanov, J. G. Körner, and V. E. Lyubovitskij, Eur. Phys. J. direct **4**, 1 (2002).
[35] F. Krüger and J. Matias, Phys. Rev. D **71**, 094009 (2005).
[36] S. Descotes-Genon, J. Matias, M. Ramon, and J. Virto, J. High Energy Phys. 01 (2013) 048.

[37] S. Descotes-Genon, T. Hurth, J. Matias and J. Virto, J. High Energy Phys. 05 (2013) 137.
[38] P. Colangelo and A. Khodjamirian, in *At the Frontier of Particle Physics: Handbook of QCD*, edited by M. Shifman (World Scientific, Singapore, 2001), p. 1495.
[39] P. Ball and R. Zwicky, Phys. Rev. D **71**, 014029 (2005).
[40] A. Khodjamirian, T. Mannel, A. A. Pivovarov, and Y.-M. Wang, J. High Energy Phys. 09 (2010) 089.
[41] M. Beneke, T. Feldmann, and D. Seidel, Nucl. Phys. **B612**, 25 (2001).
[42] B. Grinstein and D. Pirjol, Phys. Rev. D **70**, 114005 (2004).
[43] M. Beylich, G. Buchalla, and T. Feldmann, Eur. Phys. J. C **71**, 1635 (2011).
[44] C. Bourrely, L. Lellouch, and I. Caprini, Phys. Rev. D **79**, 013008 (2009); **82**, 099902(E) (2010).
[45] C. Bobeth, P. Gambino, M. Gorbahn, and U. Haisch, J. High Energy Phys. 04 (2004) 071.
[46] J. Beringer *et al.* (Particle Data Group), Phys. Rev. D **86**, 010001 (2012).
[47] UTfit Collaboration, http://www.utfit.org/.
[48] C. Bobeth, G. Hiller, and G. Piranishvili, J. High Energy Phys. 07 (2008) 106.
[49] W. Altmannshofer (private communication).
[50] D. Bećirević and A. Tayduganov, Nucl. Phys. **B868**, 368 (2013).
[51] R. Aaij *et al.* (LHCb Collaboration), J. High Energy Phys. 08 (2013) 131.
[52] R. Aaij *et al.* (LHCb Collaboration), J. High Energy Phys. 07 (2013) 084.
[53] CDF Collaboration, Public Note 10894, Version 0.1, http://www-cdf.fnal.gov/physics/new/bottom/bottom.html.
[54] S. Chatrchyan *et al.* (CMS Collaboration), Phys. Lett. B **727**, 77 (2013).
[55] ATLAS Collaboration, Report No. ATLAS-CONF-2013-038, http://cds.cern.ch/record/1537961/.
[56] R. N. Faustov and V. O. Galkin, Eur. Phys. J. C **73**, 2593 (2013).
[57] R. Aaij *et al.* (LHCb Collaboration), Phys. Rev. Lett. **111**, 112003 (2013).
[58] M. Ablikim *et al.* (BES Collaboration), Phys. Lett. B **660**, 315 (2008).